Biomedical Signal Processing and Control xxx (2016) xxx-xxx

Contents lists available at ScienceDirect

Biomedical Signal Processing and Control

journal homepage: www.elsevier.com

Research paper

Data mining framework for breast lesion classification in shear wave ultrasound: A hybrid feature paradigm

U. Rajendra Acharya [a, b, c], Wei Lin Ng [d], Kartini Rahmat [d], Vidya K. Sudarshan [a, *], Joel E.W. Koh [a], Tan Jen Hong [a], Yuki Hagiwara [a, b, c, d], Chai Hong Yeong [d], Kwan Hoong Ng [d]

[a] Department of Electronics and Computer Engineering, Ngee Ann Polytechnic, Singapore
[b] Department of Biomedical Engineering, School of Science and Technology, SIM University, Singapore
[c] Department of Biomedical Engineering, Faculty of Engineering, University of Malaya, Malaysia
[d] Department of Biomedical Imaging, Faculty of Medicine, University of Malaya, Malaysia

ARTICLE INFO

Article history:
Received 3 August 2016
Received in revised form 12 October 2016
Accepted 2 November 2016
Available online xxx

Keywords:
Elastography
Shear wave elastography
Benign breast lesions
Malignant breast lesions
Nonlinear features

ABSTRACT

Assessment of elasticity parameters of breast using ultrasound elastography (USE) provides exclusive information about the cancerous tissue. Shear wave elastography (SWE), a new USE imaging procedure is increasingly used for elasticity evaluation of breast lesions. SWE examination is gaining popularity in the characterization of benign and malignant breast lesions as it has high diagnostic performance accuracy. However, some degree of manual errors, such as probe compression or movement may cause inaccurate results. In addition, the systems cannot measure elasticity values in small lesions where the tissues do not vibrate enough. Thus, computer-aided methods suppress these technical or manual limitations of SWE during evaluation of breast lesions. Therefore, this paper proposes, a novel methodology for characterization of benign and malignant breast lesions using SWE. Original SWE image is subjected to *three* levels of Discrete wavelet transform (DWT) to obtain different coefficients. Second order statistics (Run Length Statistics) and Hu's moments features are extracted from DWT coefficients. Extracted features are subjected to sequential forward selection (SFS) method to obtain the significant features and ranked using ReliefF feature ranking technique. Ranked features are fed to different classifiers for automated characterization of benign and malignant breast lesions. Our proposed technique achieved a significant accuracy of 93.59%, sensitivity of 90.41% and specificity of 96.39% using only *three* features. In addition, a unique integrated index named ***Shear Wave Breast Cancer Risk Index (sBCRI)*** is formulated for characterization of malignant and benign breast lesion using only *two* features. The proposed index, *sBCRI*, provides a single number which characterizes the malignant and benign cancer faster. This system can be employed as an ideal screening tool as it has high sensitivity and low false-positive rate. Hence, the women with benign lesions need not undergo unnecessary biopsies.

1. Introduction

Breast cancer is one of the leading cancers (malignancies) in women and the second primary cause of cancer-associated deaths [11,56,119]. According to World Health Organization (WHO), in 2011, more than 508,000 breast cancer deaths are reported in women worldwide [112]. It is reported that, 1.8 million women are diagnosed with breast cancer worldwide in 2013 [48] and it is projected that in 2016, in the United States of America (USA) alone, approximately 246,660 new cases of invasive breast cancer will be diagnosed among women [23].

Breast cancer is the result of uncontrolled multiplication of cancer cells in the breast and commonly it begins at lobes of mammary glands [1]. This group of rapidly dividing cancer cells in the breast may eventually form a lump called as breast tumor. Breast lesion can be benign (not cancerous) or malignant (cancerous) depending on their characteristics and the degree of risk they carry [1]. Imaging of breast lesions is now regarded as essential in addition to the clinical diagnosis of breast malignancies [122]. Mammography and ultrasound (US) remain as the standard front line techniques for both screening and symptomatic disease evaluation. However, mammography performed on the dense breast may frequently produce false-negative results [22,68,69,101] and thus delay the diagnosis of cancer. Few studies have demonstrated that adding an US scan to screen women having the dense breast tissue together with a mammography can detect additional cancers per 1000 women [20,55]. Even though the US is highly sensitive [106,126] when applied to dense breast, lack specificity [19,31] resulting in an alarming number of false-positive; thus increasing the rate of unnecessary biopsies [49,101]. Report suggests that, using conventional US, it is difficult to precisely distinguish isoechoic lesions from the surrounding fat [89]. Therefore, despite of having regular screening tests, the breast cancers fail to be diagnosed at an early curable stage.

Clinically, it is essential to evaluate the lesion location surrounding tissue and the lesion characteristics such as size and shape according to the Breast Imaging-Reporting and Data System (BI-

* Corresponding author at: Department of Electronics and Computer Engineering, Ngee Ann Polytechnic, 599489, Singapore.
Email address: vidya.2kus@gmail.com (V.K. Sudarshan)

http://dx.doi.org/10.1016/j.bspc.2016.11.004
1746-8094/

RADS) criteria using either mammography or an US for characterization of malignancies [87]. The primary characteristics of breast lesions include the clarity and contour of the lesion margins, the orientation and shape of the lesion, boundary echoes, the echo texture and echogenicity [17,61,106,109]. In addition, the lesion compressibility and vascularity may also be evaluated. Benign breast lesions appear round, oval minimally lobulated in shape with intense boundary echoes and homogenous internal echoes [8,18,106]. While the malignant breast lesions appear without proper margin or boundary, and may exhibit heterogeneous echo patterns, and an increased anteroposterior dimension [106]. Breast US can be used to characterize these physiological and pathological characteristics of both palpable and nonpalpable breast lesions [18,106]. Despite this, it lacks fundamental and quantitative information on the tissue elastic properties as cancer tissue is harder, stiffer (less elastic) and less compressible compared to normal breast tissue [43,102]. Moreover, improved breast US imaging modalities such as US tomography [37,98] and multi-modal US tomography (ultrasound transmission tomography (UTT) and ultrasound reflection tomography (URT)) [94,125] are intensively becoming effective in assessing the breast lesion characteristics [94,98]. Although the initial results are promising, further work with larger set of breast cancer patients are required to demonstrate their diagnostic efficacy before clinical application [94,98].

Currently, to conquer these limitations and attain more precise lesion characterization, breast US elastography (USE) is introduced [13,15,35,54,99]. Breast USE technique is used in breast lesion assessment and characterization [60]. Numerous works testified that it can improve the B-mode US specificity in distinguishing the malignant and benign breast lesions [27,28,60]. It is used to assess the tissue deformity (elasticity) and quantify the stiffness of the tissue [60,93,103].

Among the two available USE techniques such as strain elastography (SE) and shear wave elastography (SWE), SWE is the only one that is highly reproducible [32,40,50,88]. In SWE, transversely aligned shear waves are produced by an acoustic radiation force during the application of an ultrasound probe to the tissue [77]. The waves travel faster in stiff (hard) tissues than in soft tissues [49]. For every pixel in the region of interest (ROI), it provides an image with color-code presenting the shear wave elasticity (kilopascals, kPa) or velocity (m/sec) [115]. Commonly, a color scale of 0 (dark blue) is used for the soft breast lesions and +180 kPa (red) for hard lesions [77]. In addition to the qualitative parameters (lesion and an adjacent tissue stiffness, lesion size, shape, and rim stiffness), quantitative parameters of the lesion such as mean elasticity (Emean), maximum and minimum elasticity (Emax, Emin) and elasticity ratio (Eratio) can be assessed using the SWE and are used in classification of benign and malignant breast lesions [10,67].

According to a study, elasticity parameter measured in the breast lesions (benign lesions <80 kPa and malignant lesions >100 kPa) can be a good indicator for differentiation of benign and malignant lesions [108]. Various cutoff values for the elasticity parameters such as 80 kPa [24], 30 kPa [78] and 65 kPa [21] are proposed by different studies [21,25,39]. Olgun et al. [91] assessed the minimum, mean and maximum elasticity values with different cutoff in differentiating the malignant from benign lesions using a SWE. The study results showed the sensitivity and specificity of (i) 96% and 95% for the mean elasticity with a cutoff value of 45.7 kPa, (ii) 95% and 94% for the maximum elasticity with a cutoff value of 54.3 kPa, and (iii) 96% and 95% for the minimum elasticity with a cutoff value of 37.1 kPa respectively. In general, the velocity is higher for the stiffer tissue in order for the waves to travel through them. The simple lumps produce 0 velocity, because of the presence of non-viscous fluids in which the shear waves do not travel [16]. Thus, using the SWE, the degree of tissue deformation is evaluated where the stiffer tissues infiltrated with cancer deform less and stiffer (less elastic), thereby can be easily differentiated from the normal and benign surrounding tissues [71]. Various research studies are conducted for evaluating these quantitative SWE parameters in order to differentiate the malignant breast lesions from benign breast masses [21,25,40,52,66,75,76,110,114]. Table 1 summarizes few of the studies on breast lesion identification using the SWE image parameters. In most of the studies, the SWE parameters are significantly higher for malignant breast lesions than the benign cases [21,25,39,76,110,123]. The mean stiffness elasticity has been found to be a useful parameter in yielding an accurate benign and malignant differentiation of solid masses [40]. In addition, for invasive breast cancers, it is shown that the breast lesions are stiffer compared to the normal lesions [41] and often produce areas of stiffness that are larger than the gray-scale abnormality generated by B-mode ultrasound [60].

However, often during the breast SWE assessments, difficulties are faced in inferring the significance of elasticity values, due to the various scanning angles providing different elasticity values. The reason for these difficulties is that breast lesions are heterogeneous and three dimensional structures [44]. To resolve this issue, Kim et al. [64] conducted a study for evaluating the effect of scanning angle on the diagnostic performance of the SWE in discriminating the breast malignancy from benign lesions. Results propose that the use of two orthogonal views that capture the images will increase the diagnostic performance of breast SWE.

Many recent studies suggest that the SWE improved the diagnostic performance accuracy and specificity of conventional US alone in the diagnosis of breast lesions [21], [26,40,75,76,82,110,124]. By adding SWE, about 90% of 4a masses are downgraded to BI-RADS category 3, thus, unnecessary biopsies on the benign lesions can be reduced [12,25,39,80]. However, it is observed that the small breast cancers are not as stiff as the larger cancers, indicating that the tumor size as well as the specific histological type can also affect the stiffness value [44,76]. In contrast, it has been reported that the diagnostic performance of elastography is better than the conventional US in the characterization of small masses (1 cm) [86]. Therefore, in 2015, Kim et al. [65] evaluated the diagnostic performance of SWE features combined with an US in the assessment of small ($\leq$ 2 cm) lesions. The study reported that by combining the two techniques, specificity increased and the number of unnecessary biopsies can be reduced while evaluating the small breast lesions. It is also shown that the breast lesion stiffness quantitatively measured by the SWE is a helpful predictor of under-estimated malignancy in an US-guided 14-gauge core needle biopsy (CNB) [95]. Lee et al. [79] claimed that the SWE is highly sensitive in an accurate identification of the presence of residual breast malignant lesions even after a neoadjuvant chemotherapy (NAC) and showed an improved diagnostic performance (sensitivity 83.6% and specificity 80%) compared to the B-mode US (sensitivity 72.1% and specificity 50%).

Recently in 2016, Ng et al. [90] investigated the efficiency of the SWE in classifying benign and malignant using 159 SWE breast lesions images. The experimental results presented 100% sensitivity and 97.6% specificity with a cutoff value of $\geq$ 56 kPa for the maximum stiffness in detecting malignant lesions. In addition, their experiment claimed that, if the maximum stiffness cutoff value is kept $\geq$ 80 kPa, 95.5% of BI-RADS 4a lesions can be downgraded to BI-RADS 3, thereby negating the need for the biopsy. Even though, the SWE technique is classically less operator-dependent, some degree of variability may occur if too much pressure is applied to the

Table 1
Summary of studies on breast lesion identification using the SWE image parameters.

Author (year)	Data	Methods/Features	Classification	Findings/Results
Evans et al., [40]	Ultrasound with SWE Subjects: 52 patients (23 benign and 30 malignant lesions).	Emean	Statistical Analysis	Accuracy = 91% Sensitivity = 97% Specificity = 83%
Chang et al., [25]	Ultrasound and SWE Subjects: 158 women with 182 breast lesions (89 malignant, 93 benign)	Emean	Statistical Analysis	Cutoff 80.17 kPa: Accuracy = 86.8% Sensitivity = 88.8% Specificity = 84.9%
Evans et al., [39]	BI-RADS ultrasound and SWE Subjects: 173 women with 175 breast lesions (64 benign and 111 malignant)	Emean, Emax	Statistical Analysis	SWE alone: Accuracy = 89% Sensitivity = 95% Specificity = 77% SWE and BI-RADS US combined: Accuracy = 86% Sensitivity = 100% Specificity = 61%
Chang et al., [24]	Ultrasound, SWE and strain Elastography 150 breast lesions (71 malignant, 79 benign)	Emean and SD	Statistical analysis and ROC	Ultrasound: Sensitivity = 100% Specificity = 19% SWE: Sensitivity = 95.8% Specificity = 84.8% Strain Elastography: Sensitivity = 81.7% Specificity = 93.7%
Youk et al., [52]	Ultrasound and SWE Subjects: 389 breast masses (269 benign and 120 malignant)	SWE features: Eratio, Emin, Emax, Emean US features: Diameter and depth of lesion, distance from the nipple.	Chi-auqare and Mann-Whitney *U* test	Eration (5.14 cutoff): Sensitivity = 88% Specificity = 90.6%
Lee et al., [76]	Ultrasound and 2D and 3D SWE Subjects: 134 women with 144 breast lesions (67 malignant)	Emax, Emean, Eratio	ROC statistical analysis	2D and 3D SWE = improved specificity of ultrasound from 29.9% to 71.4%.
Youk et al., [115]	Ultrasound with SWE Subjects: 123 patients with 130 breast lesions (49 malignant and 81 benign)	Emean, Emax, SD and wSD (SD of elasticity of the whole breast lesion) measured in kPa and m/sec	AUC of ROC	AUC for the wSD = 0.964 kPa and 0.960 m/sec Specificity of SD using kPa and m/sec = 95.1% vs 87.7%
Youk et al., [116]	Ultrasound, strain elastography and SWE Subjects: 79 breast lesions	Qualitative and quantitative (SWE parameters) parameters	Statistical analysis	SWE: 56% of category 4a lesions were downgraded.
Lee et al., [78]	Ultrasound and SWE Development cohort: 159 breast masses (21 malignant) Validation cohort: 207 breast masses (12 malignant)	Emax	t-test	Reported increase in specificity.
Olgun et al., [91]	Ultrasound and SWE Subjects: 109 patients with 115 lesions (83 benign and 32 malignant)	Emin, Emean, Emax, mass/fat Eratio	Statistical Analysis - SPSS	Emean (45.7 kPa cutoff): sensitivity = 96%, specificity = 95% Emax (54.3 kPa cutoff): sensitivity = 95%, Specificity = 94% Emin (37.1 kPa cutoff): Sensitivity = 96% Specificity = 95% Mass/fat Eratio: Sensitivity = 97% Specificity = 95%
Au et al., [12]	Ultrasound and SWE Subjects: 112 women with 123 masses (79 benign and 44 malignant)	Emean, Emax, Eratio	Statistical Analysis - SPSS	Eratio (3.56 cutoff) Combined ultrasound and SWE: Accuracy = 90.24% Specificity = 87.34% By adding SWE parametrs to BI-RADS category 4a masses, about 90% of them could be correctly downgraded to category 3, thereby avoiding biopsy.
Kim et al., [65]	Ultrasound with SWE Subjects: 171 patients with 177 small breast lesions (22 malignant and 155 benign)	SWE parameters − Emean, Emax, Eratio	Statistical analysis - SPSS	Emax (cutoff 87.5 kPa) Sensitivity = 68.2% Specificity = 87.1%
Lee et al., [79]	Ultrasound with SWE and MRI data Subjects: 71 patients with breast cancers	Emax	ROC	Ultrasound alone: Accuracy = 69% Sensitivity = 72.1% Specificity = 50% SWE alone: Accuracy = 83.1% Sensitivity = 83.6% Specificity = 80% Ultrasound and SWE: ROC = significantly high than that of ultrasound alone

Table 1 (*Continued*)

Author (year)	Data	Methods/Features	Classification	Findings/Results
Lee et al., [80]	Ultrasound and SWE Subjects: 139 patients with 140 breast lesions (30 malignant)	SWE parameters	Statistical Analysis	Emax (cutoff 108.5 kPa) Sensitivity = 86.7% Specificity = 97.3%
Xian-Quan et al., 2015	Ultrasound and SWE Subjects: 302 breast lesions	Emax, Emean, Emin, Esd, Eratio	Statistical Analysis	SWE: Emax: Sensitivity = 87% Specificity = 97%
Ng et al., [90]	Ultrasound with SWE Subjects: 159 breast lesions (85 benign, 74 malignant)	SWE parameters − Maximum elasticity (Emax), Mean elasticity (Emean), minimum elasticity (Emin), Ratio of lesion elasticity to surrounding tissue (Eratio), SD	Statistical analysis - SPSS	Sensitivity = 100% Specificity = 97.6% using Emax parameter in detecting malignant lesions
Choi et al., [29]	Ultrasound and SWE Subjects: 81 non-mass lesions (74 malignant and 7 benign)	SWE: Emax, Emean and maximum stiffness color US: Lesion size	t-test Chi-square test Fisher's exact test	SWE: Emean (85.1 kPa cutoff) Accuracy = 84.5% Sensitivity = 78.4% Specificity = 95.2% Emax (92.5 kPa) Accuracy = 83.6% Sensitivity = 78.4% Specificity = 92.9% US + SWE: Emean (85.1 kPa or high vascularity): Accuracy = 84.5% Sensitivity = 95.9% Specificity = 64.3%
Li et al., [82]	Ultrasound and SWE Subjects: 276 patients with 296 breast lesions (212 benign and 84 malignant)	SW velocity	Statistical Analysis	SWE alone: Sensitivity = 67.9% Specificity = 86.3%
Computer-Aided Diagnostic System				
Lo et al., [83]	US and SWE Subjects: 57 benign and 31 malignant tumors	18 SWE features (mean, variance, skewness, kurtosis, density, average from RGB color patterns)	Logistic regression classifier	SWE: Accuracy = 81% Sensitivity = 61% Specificity 91%
Zhang et al., [121]	Ultrasound and SWE Subjects: 125 women with 161 breast tumors	Contourlet-based texture features (Tmean, Tamx, Tmedian, Tqt − third quartile, Tsd − standard deviation of the sub bands) − first order statistics	ROC and Fisher classifier	Accuracy = 92.5% Sensitivity = 89.1% Specificity = 94.3%

probe [13]. Thus, the reliability of the SWE method depends on the operator's training and experience, if neglected, technical errors such as probe movement or compression can cause inaccurate results [32,52,88]. Moreover, manual evaluation of the SWE parameters is time-consuming and prone to errors [13]. Therefore, in order to overcome these manual or technical errors, the computer-aided methods are required for the benign and malignant breast SWE image characterization.

In 2015, Lo et al. [83], proposed a computer-aided diagnosis (CAD) tool to assess the breast lesions using SWE images. First order statistics based features such as mean, variance, kurtosis, skewness and density of the different color channels (Red, Green, and Blue − RGB) are extracted from the tumor ROIs of the SWE. Furthermore, these features from the 3 color channels are merged as a vector to assess the tissue elasticity. The study reported that the SWE parameters showed an accuracy of 81% in classification of BI-RADS 2, 3, 4, 5 breast lesions and 83% in classification of only BI-RADS 4 category breast lesions using a logistic regression classifier. Zhang et al. [121] assessed the elastic heterogeneity of breast tumors in the SWE using contourlet-based texture analysis. They extracted the first order statistical features (Tmean, Tmaximum, Tmedian, Tthird quartile and Tstandard deviation) from the directional sub bands after the contourlet transform. Their study reported 92.5% accuracy, 89.1% sensitivity and 94.3% specificity in the classification of benign and malignant breast tumors. However, first order statistical features cannot capture the higher–order interrelationships present in the images. Therefore, there is a need for second-order or higher-order and/or nonlinear feature extraction methods to capture the subtle changes occurring within the images [85].

It is evident from the literature review (Table 1) that few researchers [83,121] have proposed an automated benign and malignant breast lesion classification system using the SWE images. In view of this, in this work, a unique algorithm for an automated characterization of the benign and malignant breast lesions using SWE images is proposed. Fig. 1 shows the block diagram of our proposed algorithm. Novelty of our proposed system is the formulation of a ***Shear Wave Breast Cancer Risk Index (sBCRI)*** for the classification of benign and malignant breast lesions. Initially, the Discrete Wavelet Transform (DWT) is performed on the SWE images up to *three* levels to obtain different coefficients. From these DWT coefficients, various second order statistics using Run Length Statistics (RLS) and Hu's moments are extracted and subjected to sequential forward selection (SFS) method. The significant features obtained are ranked using ReliefF algorithm. All the ranked features are subjected to decision tree (DT), K nearest neighbor (KNN), linear discriminant analysis (LDA), quadratic discriminant analysis (QDA), support vector machine (SVM), and probabilistic neural network (PNN) classifiers for the automated characterization of benign and malignant. The performance of these classifiers are tested using 10-fold cross validation method.

2. Data collection

The data for the current study were obtained from the Department of Biomedical Imaging, University of Malaya Medical Centre (UMMC), Malaysia. The necessary institutional medical ethics committee board approval was obtained for this study. The patients were recruited from June 2012 to April 2013 by obtaining the informed consent before their recruitment. All the patients recruited were having breast lesions of BIRADS 4 category and above, and were even scheduled for ultrasound core biopsy. A total of 156 patients (73 with malignant and 83 with benign) were recruited with either palpable lumps or sonographycally detected lesions. All scans were performed using the Aixplorer ultrasound system (SuperSonic Imagine, Aixen Provence, France) using a 15–4 MHz linear transducer probe. Initially, B-mode gray scale images were captured using ultrasound alone and about 3–5 min later, elastography images were generated using SWE method [90].

Fig. 1. Block diagram of proposed algorithm.

3. Methodology

3.1. Pre-processing

The images are cropped (about 195 × 195 resolution) to have only the SWE 3 × 3 cm color map in transverse plane placed on the region encompassing the lesions and its immediate surrounding tissues. Later, the red-green-blue (RGB) color SWE images are converted into grayscale and the contrast of these images are enhanced by using adaptive histogram equalization [51].

3.2. Feature extraction

This stage is essential for the interpretation of abnormal and normal classes. The second order statistics RLS and Hu's moments techniques are implemented in this work to analyze the SWE images. Various RLS and Hu's moments features are evaluated from the DWT coefficients of SWE breast images. The detailed proposed methodology is explained in this section.

3.2.1. Discrete wavelet transform (DWT)

This technique converts the time domain signal into wavelet domain to obtain the time and frequency values in terms of coefficients [9,92]. Filter banks are used to decompose the images into high-pass (detail) and low-pass (approximation) components [84].

By decomposing the original image using high- and low-pass filters, *four* sub band images *LL*, *LH*, *HL*, and *HH* are obtained. The *LL* coefficients signify the total energy in an image and are called approximation coefficients. The detail coefficients *HL*, *LH,* and *HH* are vertical, horizontal, and diagonal details of the image respectively. The approximation coefficients are further decomposed to obtain the second-level sub band image. These individual sub bands represented as $HDCL_i$, $VDCL_i$, $DDCL_i$, *and* $ADCL_i$ are the horizontal, vertical, diagonal and approximation coefficients acquired at the i^{th} level decomposition respectively [34]. In this work, DWT is performed on the SWE of benign and malignant images up to *three* levels using biorthogonal 3.1 (bior3.1) mother wavelet function [2]. Fig. 2 shows the *three* level DWT coefficients of benign and malignant SWE images.

It can be seen from Fig. 2 that, there is distinct variation in the pixels of benign and malignant DWT sub bands. The sub bands of malignant lesion exhibit more sudden variations as compared to benign may be due to the sudden changes in the pixels. We have extracted different features from these DWT coefficients of various sub bands.

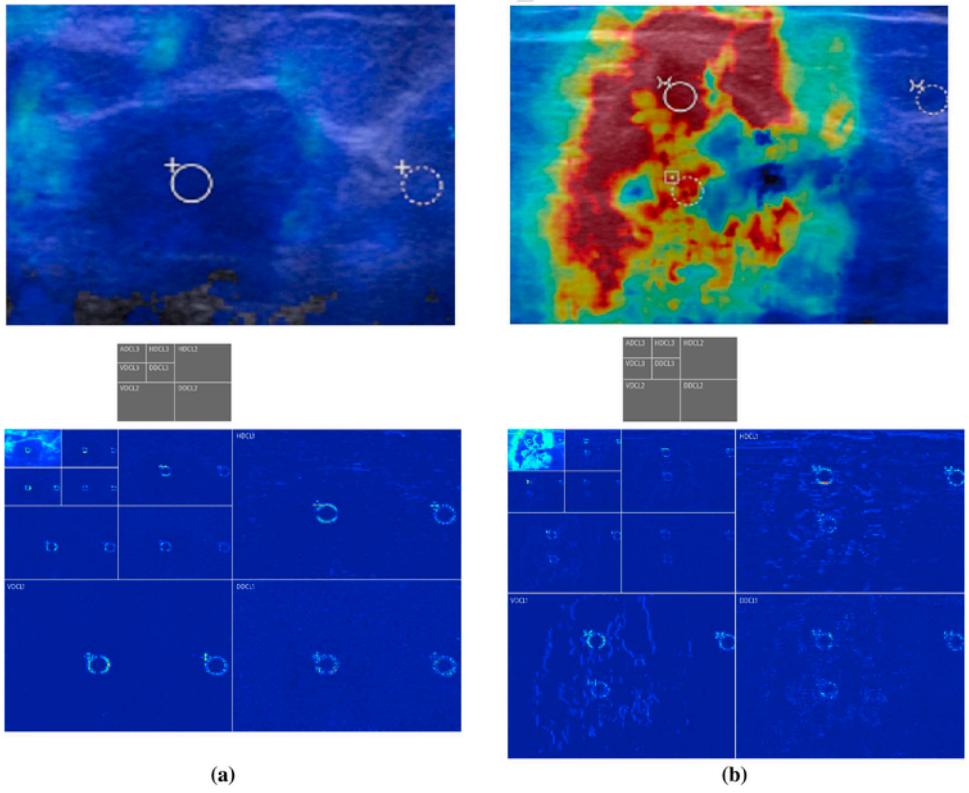

Fig. 2. Three-level sub-bands of 2D DWT (bottom row) of SWE images (top row): (a) benign and (b) malignant.

3.2.2 Gy level run-length matrix (GLRLM) or run-length statistics (RLS)

Galloway et al. [42] introduced the idea of RLS to capture the details of an image from its gray level runs. Set of image points with similar gray levels are represented by gray level run. In that run, the count of image points is a length of the run. A run-length matrix $p(i, j)$ stores information of the count of runs with pixels of gray level i and run length j. With M representing the number of gray levels, N the number of runs, $N_r$the number of different run lengths, and N_g the number of gray levels and P the number of pixels in the image respectively, the Short runs emphasis (sR_E^x),Gray level non-uniformity (GL_{-u}^x), Long runs emphasis (lR_E^x), Run length non-uniformity (RL_{-u}^x) and Run percentage (R_P^x) features are extracted using RLS methods.

Chu et al. [30] proposed a new technique based on the gray value distribution of the runs and defined 2 different features Low gray-level run emphasis ($lGLR_E^x$) and High gray-level run emphasis ($hGLR_E^x$). Dasarathy et al. [33] proposed a new method for the image characterization based on the idea of joint gray level and run length distributions. The four features Short run low gray-level emphasis ($sRlGL_E^x$), Short run high gray-level emphasis ($sRhGL_E^x$), Long run high gray-level emphasis ($lRhGL_E^x$) and Long run low gray-level emphasis ($lRlGL_E^x$) proposed by this method are extracted.

3.2.3. ***Hu's moments*** *(Hu_m^x)*

In this work, seven moments (Hu_m^x, where $m = 1, 2, 3, ...7$) developed by Hu which are invariant to rotation, scaling and translation variations of the images are extracted [3], [57]. These moments capture the details about intensity distribution, geometrical (shape) features and helps to identify the patterns in images [57], [120].

3.3. Feature selection and ranking

All nonlinear features assessed are not capable of classifying the benign and malignant groups. Thus, to recognize the extremely resourceful features with useful information, sequential forward feature selection method is used. The Sequential forward selection (SFS) selects the features sequentially and adds to an empty sub set until the addition of features maximizes the classification accuracy [70], [81]. The main advantages of using this SFS method is its computational efficiency and avoids over fit [72]. In addition, this SFS method of feature selection has frequently shown to perform competitively compared to other method like sequential floating forward selection (SFFS) [96], [97]. Thus, this method is considered as one of the state-of-the-art feature selection techniques. Selected features are subjected to ReliefF feature ranking method which uses the k nearest neighbors − hits (from the same class) and misses (from the different class). The averages of their contributions are added to Relief's estimate [100].

3.4. Classification

Classification is performed on the ranked features using different classifiers in order to attain the maximum outcome. In this work, DT, LDA, QDA, SVM Polynomial 1, 2, 3 and RBF, PNN and KNN classifiers are experimented to find the best classifier in distinguishing the benign and malignant SWE images [36]. ***DT*** classifier, builds a tree from the features during the training phase [73]. Based on the rules obtained from the tree it built, classifies the two classes and thereby identifies the class of test (unknown) data. ***KNN*** classifier determines k-nearest neighbors i.e. the minimum distance between training and testing data [74]. The unknown sample gets the most common class among the k-nearest neighbors. ***SVM*** classifier in the higher-dimensional space constructs a separating hyperplane which splits the training sets into two classes [38]. In this work, we have used polynomial 1, 2, 3 and RBF kernel functions. ***PNN*** classifier works on the principle of supervised learning algorithm and calculates the weights. Using a multi-layered neural network having 4 layers, this classifier is often employed in classification of two groups [111]. Two types of ***discriminant classifiers*** such as LDA and QDA are employed in this work. LDA and QDA learns from linear and quadratic boundaries respectively [59], [63]. A 10-fold cross validation technique is employed in our work for performance validation of the classifiers.

4. Results

4.1. Results of feature extraction

The results of feature extraction and classification are presented in this section. Each SWE image is subjected to *three* level DWT to obtain a total of 12 DWT coefficients. Total of 216 (12 DWT coefficients X (11 RLS + 7 Hu's moments)) features are computed. All together 216 × 156 features are computed from both benign and malignant breast lesions.

Table 2 shows the *mean* and standard deviation (SD) values of second order (RLS) and nonlinear (Hu's moments) features extracted from the DWT coefficients of benign and malignant SWE images. Significant features selected using SFS method are ranked by ReliefF technique and the best 3 highly ranked features are tabulated in Table 2 and Fig. 3.

It is evident from Table 2 and Fig. 3 that the feature values are higher in malignant lesions compared to the benign lesions. This is may be due to the more abrupt changes in the pixels of malignant lesion. In benign lesion, the pixel variations are less abrupt as compared to malignant contributing to the smaller values.

4.2. Results of classification

Ranked features are fed to different classifiers namely, DT, LDA, QDA, SVM, KNN and PNN to achieve the highest classification performance. QDA classifier has achieved the maximum accuracy, sensitivity and specificity of 93.59%, 90.41% and 96.39% respectively using the DWT method with *three* features ($RL_{-u}^{A1}, RL_{-u}^{H1}, Hu_5^{H1}$). Table 3 shows the results of classification obtained using second-order statistics, RLS and Hu's moments. It is evident from this Table 3 that the QDA outperformed other classifiers in achieving the highest results.

We have also performed classification without the DWT using only RLS and Hu's moments directly from the SWE images. We have achieved 88.46% accuracy, 83.56% sensitivity and 92.77% specificity using only *two* features. Therefore, extracting features (RLS and Hu's moments) from the DWT coefficients has significantly improved the classification performance. Thus, fusion of three techniques DWT, RLS and Hu's moments showed better results in an efficient characterization of the benign and malignant breast lesions from SWE images.

4.3. Results of index − sBCRI

Apart from the classifiers, an idea of integrated index, first introduced by Ghista [45], [46,47], is proposed for the characterization of benign and malignant breast lesions in this work. An integrated index

Table 2
Results (mean ± SD) of top three features extracted from benign and malignant breast SWE images using RLS and Hu's moments methods.

Features	Benign		Malignant		*p*-Value	Criterion
	Mean	SD	Mean	SD		
RL_{-u}^{A1}	2.10E + 03	1.78E + 02	1.59E + 03	2.35E + 02	0.0000	0.0229
RL_{-u}^{H1}	3.57E + 02	1.16E + 02	4.15E + 02	1.46E + 02	0.0067	0.0083
Hu_5^{H1}	6.81E + 01	2.16E + 01	8.08E + 01	3.03E + 01	0.0028	0.0048

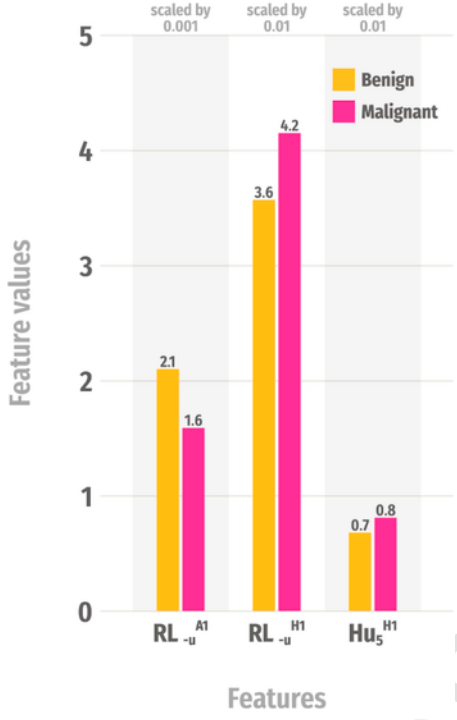

Fig. 3. Bar plots of mean values of extracted features from benign and malignant SWE images using RLS and Hu's moments method.

Table 3
Results of classification of benign and malignant SWE image features obtained using RLS and Hu's moments methods.

Classifiers	NOF	TP	TN	FP	FN	Acc (%)	Sen (%)	Spe (%)
DT	3	62	76	7	11	88.46	84.93	91.57
LDA	3	64	81	2	9	92.95	87.67	97.59
QDA	3	66	80	3	7	93.59	90.41	96.39
SVM Poly 1	3	64	81	2	9	92.95	87.67	97.59
SVM Poly 2	3	62	80	3	11	91.03	84.93	96.39
SVM Poly 3	3	66	78	5	7	92.31	90.41	93.98
KNN − 25	3	63	82	1	10	92.95	86.30	98.80
PNN − 0.15	2	61	82	1	12	91.67	83.56	98.80
SVM RBF − 1.4	3	66	79	4	7	92.95	90.41	95.18

Acc = accuracy; Sen = sensitivity; Spe = specificity; TP = true positive; TN = true negative; FP = false positive; FN = false negative; NOF = number of features.

named *sBCRI* is formulated by merging the most distinctive features in such a way that the index value is noticeably different for the two classes.

In the current work, a *sBCRI* is formulated using the two features such as RL_{-u}^{A1} and Hu_5^{H1} obtained from the SWE images (Table 2). These two features are then combined (see Eq. (1)) to produce an index which is highly distinguishing. Mathematical equation of this *sBCRI* is given as,

$$sBCRI = \frac{\left(1.5 \times \left(RL_{-u}^{A1}\right) + 2.2 \times \left(Hu_5^{H1}\right) + 5.5\right)}{1000} \quad (1)$$

This *sBCRI* formulated gives a maximum distinction between the two classes (benign and malignant). Table 4 shows the *sBCRI* values for the subjects with malignant and benign breast lesions. A plot of *sBCRI* for the benign and malignant cases obtained using the combination of two features (RL_{-u}^{A1} and Hu_5^{H1}) is shown in Fig. 4. Thus, *sBCRI* (a single number) aids the clinicians in faster and an accurate characterization of the benign and malignant breast lesions.

5. Discussion

In this work, a unique algorithm is proposed by fusing DWT, texture and Hu's moments features. DWT method decomposes SWE image into the sets of images at different positions and scales by using filter banks. Hence this time-invariant decomposition method (DWT) is very effective in separating noise from an image [62,107]. An important benefit of this method is its ability to treasure temporal resolution of the images; in other words, it captures both frequency and location details [6,84]. Furthermore, DWT technique is robust and useful in detecting irregularities present in the images [4,6,7]. Thus, DWT multiresolution analysis technique is advantageous for obtaining an efficient performance using the SWE images.

Several other researchers have analyzed the SWE images using quantitative parameters [21,25,40,64,66,76,90,110], texture features

Table 4
Range of a *sBCRI* for the benign and malignant breast lesions.

Benign		Malignant	
Mean	SD	Mean	SD
3.306607	0.27379	2.570718	0.367312

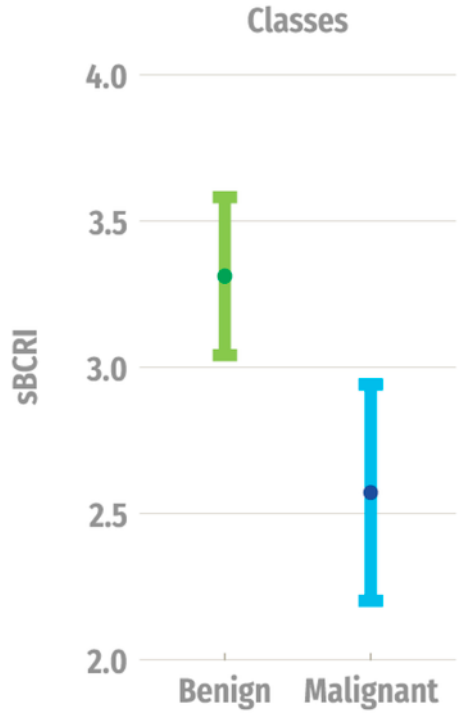

Fig. 4. Plot of sBCRI for benign and malignant breast lesions.

[83,121] in the characterization of benign and malignant breast lesions. Manual evaluation of breast lesion parameters using SWE is prone to errors during data acquisition and visual interpretation variabilities present in different USE equipment manufacturers [13,104]. An elasticity sometimes cannot be calculated when the deformation of tissue is too low. This may occur in large very rigid infiltrative cancers [110]. The systems cannot measure the elasticity values in lesions where tissue does not vibrate enough or the amplitude of shear wave is too low and thus lost in the background noise [14]. Chances of having more false positive is high for large size lesion and thick breast, and more false-negative values for the smaller and deeper lesions [114].

Thus, analysis of the image texture characteristics using computer-aided technique may overcome these limitations of manual evaluation of SWE parameters. Moreover, the high quality SWE images have shown an improved diagnostic performance in characterizing the malignant breast lesions from benign ones [25,76]. Hence, there is a need for an efficient image pre-processing technique before extraction of the features.

Hence, to surpass the obstacles, a novel technique for an automated characterization of the benign and malignant breast lesions from SWE images is proposed in this work. DWT is performed on the benign and malignant SWE images. Various RLS and Hu's moments features are computed from the DWT coefficients. Significant features are selected from the extracted parameters using SFS method. All these selected features are ranked according to the ReliefF ranking method. Later, the ranked features are classified using different classifiers. In addition, an index called *sBCRI* is formulated and developed using the second-order RLS and nonlinear Hu's moments features extracted from the SWE images for characterization of malignant and benign breast lesions. Our proposed method showed 93.59% accuracy, 90.41% sensitivity and 96.39% specificity in characterizing the benign and malignant breast lesions using only *three* ($RL_{-u}^{A1}, RL_{-u}^{H1}, Hu_5^{H1}$) features extracted from the DWT coefficients (approximation and horizontal). We have also performed the classification using same features without DWT technique. Results showed low performance in the characterization of malignant and benign as compared to the DWT technique. Therefore, fusion of DWT technique exhibited the highest performance in the characterization of malignant and benign SWE images.

Moreover, the second-order and nonlinear features (RLS and Hu's moments) used in this work are capable of extracting the spatial interrelationships and complexity present in pixels of images [5,118]. Second order statistics evaluate the properties of more than one pixel values at specific positions relative to each other [105]. The second order statistics calculated using RLS method provides for each sample the large set of features, thus, even small variations (subtle changes) occurring in an image texture are captured by these features [53,105]. Hu's moments are widely used in image pattern recognition due to its invariant nature of image translation, scaling and rotation [57,58]. Moreover, these features (RLS and Hu's moments) evaluated from the DWT coefficients provide information related to the different frequency bands present in an image [5,118]. Therefore, in essence, the second-order statistics and nonlinear features are suitable for obtaining information from the SWE images and can be successfully used for the development of an efficient diagnostic system.

In comparison to the other published studies, our proposed method achieved better sensitivity and specificity in differentiating the malignant and benign SWE images. This proposed technique can assist, if used in hospitals or polyclinics to diagnose the malignancy accurately and hence avoid the unnecessary biopsies as it has high specificity. The main novelty of our proposed work is the formulation of ***an integrated index sBCRI*** for the characterization of malignant breast lesions using only the *two* features extracted from SWE images. In future work, we will be exploring to develop an automated system using SWE for the characterization of benign, pre-malignant and malignant breast lesions.

6. Conclusion

Automated characterization of breast malignancy from benign lesions using SWE is a challenging task. In this paper, an ***integrated index, sBCRI***, for an automated characterization of breast malignant lesions is proposed. DWT technique performed on SWE images has achieved the high accuracy, sensitivity and specificity of 93.59%, 90.41% and 96.39% respectively using *three* features in the characterization of malignant and benign lesions. The proposed technique is reliable and promising. In addition, our system is affordable to the clinicians without the need for any special hardware setup. Thus, this software can be incorporated in the routine clinical practice as a screening tool to diagnose the breast lesions.

Uncited references

[29,109,113,116,117].

Acknowledgments

This project was partly funded by the institutional research grants from the University of Malaya (BK027-2012 and RP008B-13HTM). The authors would like to acknowledge the scientific committee members of the University of Malaya Research Imaging Centre (UMRIC) for reviewing the research proposal and contributing constructive comments. We would also like to thank the sonographers, Ms. Sook Sam Leong, Ms. Norhana Mohd Noor, Ms. Suziela Mohamad and Ms. Johanna Wong for their helps in ultrasound imaging.

References

[1] M.D. Abeloff, A.C. Wolff, B.L. Weber, et al., Cancer of the Breast, in: M.D. Abeloff, J.O. Armitage, A.S. Lichter, et al. (Eds.), Clinical Oncology, 4th ed.Elsevier, Philadelphia, Pa, 2008, pp. 1875–1943.

[2] U.R. Acharya, S.S. Vinitha, M.R.K. Krishnan, F. Molinari, W. Zieleznik, R.H. Bardales, A. Witkowska, J.S. Suri, Computer-aided diagnostic system for detection of hashimoto thyroiditis on ultrasound images from a Polish population, J. Ultrasound Med. 33 (2014) 245–253.

[3] U.R. Acharya, M.R.K. Mookiah, S.S. Vinitha, R. Yanti, R.J. Martis, L. Saba, F. Molinari, S. Guerriero, J.S. Suri, Evolutionary algorithm-based classifier parameter tuning for automatic ovarian cancer tissue characterization and classification, Ultraschall Medizin − Eur. J. Ultrasound 35 (2014) 237–245.

[4] U.R. Acharya, M.R.K. Mookiah, J.E.W. Koh, J.H. Tan, K. Noronha, S.V. Bhandary, A.K. Rao, Y. Hagiwara, K.C. Chua, A. Laude, Novel risk index for the identification of age-related macular degeneration using radon transformation and DWT features, Comput. Biol. Med. 73 (2016) 131–140.

[5] U.R. Acharya, N. Kannathal, L.M. Hua, L.M. Yi, Study of heart rate variability signals at sitting and lying postures, J. Bodywork Movement Ther. 9 (2) (2005) 134–141.

[6] U.R. Acharya, O. Faust, S. Vinithasree, M. Filippo, S.S. Jasjit, Thyroscreen system: high resolution ultrasound thyroid image characterization into bening and malignant classes using novel combination of texture and discrete wavelet transform, Comput. Methods Programs Biomed. 107 (2012) 233–241.

[7] S. Adamczak, W. Makiela, K. Stepien, Investigating advantages and disadvantages of the analysis of a geometrical surface structure with the use of Fourier and wavelet transform, Metrol. Meas. Syst. XVII (2010) 233–244.

[8] D.D. Adier, D.L. Hyde, D.M. Ikeda, Quantitative sonographic parameters as a means of distinguishing breast cancers from benign solid breast masses, J. Ultrasound Med. 14 (1991) 661–664.

[9] P.S. Addison, Wavelet transforms and the ECG: a review, Physiol. Meas. 26 (2005) R155–R199.

[10] S.M.I. Alhabshi, K. Rahmat, N. Abdul Halim, Semi-quantitative and qualitative assessment of breast ultrasound elastography in differentiating between malignant and benign lesions, Ultrasound Med. Biol 39 (2013) 568–578.

[11] American Cancer Society (ACS), Breast cancer facts and figures. 2003–2004.

[12] F.W.F. Au, S. Ghai, H. Moshonov, H. Kahn, C. Brennan, H. Dua, P. Crystal, Diagnostic performance of quantitative shear wave elastography in the evaluation of solid breast masses: determination of the most discriminatory parameter, AJR Am. J. Roentgenol. 203 (2014) 328–336.

[13] C. Balleyguier, S. Canale, H.W. Ben, P. Vielh, E.H. Bayou, C. Uzan, C. Bourgier, C. Dromain, Breast elasticity: principles, technique, results: an updated and overview of commercially available software, Eur. J. Radiol. 82 (2013) 427–434.

[14] R.G. Barr, Sonographic breast elastography: a primer, J. Ultrasound Med. 31 (2012) 773–783.

[15] R.G. Barr, S. Destounis, L.B. Lackey II, W.E. Svensson, C. Balleyguier, C. Smith, Evaluation of breast lesions using sonographic elasticity imaging, J Ultrasound Med 31 (2012) 281–287.

[16] R.G. Barr, Shear wave imaging of the breast: still on the learning curve, J. Ultrasound Med. 31 (2012) 347–350.

[17] L.W. Bassett, Imaging of breast masses Radiolo, Clin. North Am. 38 (2000) 669–691.

[18] S.R. Benson, J. Blue, K. Judd, J.E. Harman, Ultrasound isnow better than mammography for the detection of invasive breast cancer, Am. J. Surg. 213 (2004) 889–894.

[19] W.A. Berg, Supplemental screening sonography in dense breasts, Radiol. Clin. North Am. 42 (2004) 845–851.

[20] W.A. Berg, J.D. Blume, J.B. Cormack, E.B. Mendelson, D. Lehrer, M. Bohm-Velez, E.D. Pisano, R.A. Jong, W.P. Evans, M.J. Morton, M.C. Mahoney, L.H. Larsen, R.G. Barr, D.M. Farria, H.S. Marques, K. Boparai, Combined screening with ultrasound and mammography vs mammography alone in women at elevated risk of breast cancer, JAMA 299 (2008) 2151–2163.

[21] W.A. Berg, D.O. Cosgrove, C.J. Doré, F.K. Schäfer, W.E. Svensson, R.J. Hooley, R. Ohlinger, E.B. Mendelson, C. Balu-Maestro, M. Locatelli, C. Tourasse, B.C. Cavanaugh, V. Juhan, A.T. Stavros, A. Tardivon, J. Gay, J.P. Henry, C. Cohen-Bacrie, Shear-wave elastography improves the specificity of breast US: the BE1 multinational study of 939 masses, Radiology 262 (2012) 435–449.

[22] N.F. Boyd, H. Guo, L.J. Martin, L. Sun, J. Stone, E. Fishell, A.R. Jong, G. Hislop, A. Chiarelli, S. Minkin, M.J. Yaffe, Mammographic density and the risk and detection of breast cancer, N. Engl. J. Med. 356 (2007) 227–236.

[23] Breast Cancer Statistics, 2016. Retrieved from http://www.breastcancer.org/symptoms/understand_bc/statistics.

[24] J.M. Chang, J.K. Won, K.B. Lee, I.A. Park, A. Yi, W.K. Moon, Comparison of shear-wave and strain ultrasound elastography in the differentiation of benign and malignant breast lesions, AJR Am. J. Roentgenol. 201 (2013) W347–W356.

[25] J.M. Chang, W.K. Moon, N. Cho, S.K. Kim, Breast mass evaluation: factors influencing the quality of US elastography, Radiology 259 (2011) 59–64.

[26] L. Chen, J. He, G. Liu, K. Shao, M. Zhou, B. Li, X. Chen, iagnostic performances of shear-wave Elastography for identification of malignant breast lesions: a meta-analysis, Jpn. J. Radiol. 32 (2014) 592–599.

[27] N. Cho, M. Jang, C.Y. Lyou, J.S. Park, H.Y. Choi, W.K. Moon, Distinguishing benign from malignant masses at breast US: combined US elastography and color Doppler US-influence on radiologist accuracy, Radiology 262 (2012) 80–90.

[28] N. Cho, W.K. Moon, J.S. Park, J.H. Cha, M. Jang, M.H. Seong, Nonpalpable breast masses: evaluation by US elastography, Korean J. Radiol 9 (2008) 111–118.

[29] J.S. Choi, B.K. Han, E.Y. Ko, E.S. Ko, J.H. Shin, G.R. Kim, Additional diagnostic value of shear wave elastography and color Doppler US for evaluation of breast non-mass lesions detected at B-mode US, Eur. Radiol. (2016) http://dx.doi.org/10.1007/s00330-015-4201-6.

[30] A. Chu, C.M. Sehgal, J.F. Greenleaf, Use of gray value distribution of run lengths for texture analysis, Pattern Recogn. Lett. 11 (1990) 415–420.

[31] V. Corsetti, A. Ferrari, M. Ghirardi, R. Bergonzini, S. Bellarosa, O. Angelini, C. Bani, S. Ciatto, Role of ultrasonography in detecting mammographically occult breast carcinoma in women with dense breasts, Radiol. Med. 111 (2006) 440–448.

[32] D.O. Cosgrove, W.A. Berg, C.J. Dore, D.M. Skyba, J.P. Hendry, J. Gay, C. Cohen-Bacrie, Shear wave elastography for breast masses is highly reproducible, Eur Radiol 22 (2012) 1023–1032.

[33] B.R. Dasarathy, E.B. Holder, Image characterizations based on joint gray-level run-length distributions, Pattern Recogn. Lett. 12 (1991) 497–502.

[34] I. Daubechies, Ten Lectures on wavelet Society for industrial and applied mathematics, Philadelphia, PA, USA, 1992.

[35] M.M. Doyley, K.J. Parker, Elastography: general principles and clinical applications, Ultrasound Clin. 9 (2014) 1–11.

[36] R.O. Duda, Peter E Hart, G.S. David, Pattern Classification, Wiley-Interscience, 2012.

[37] N. Duric, P. Littrup, C. Li, O. Roy, S. Schmidt, R. Janer, X. Cheng, J. Goll, O. Rama, L. Bey-Knight, W. Greenway, Breast ultrasound tomography: bridging the gap to clinical practice, Proceedings of SPIE ?The International Society for Optical Engineering (2012).

[38] E.O. Edgar, F. Robert, G. Federico, Support Vector Machines: Training and Applications, Technical Report, MIT AI Lab Centre for Biological and Computational Learning, 1997.

[39] A. Evans, P. Whelehan, K. Thomson, K. Brauer, L. Jordan, C. Purdie, D. McLean, L. Baker, S. Vinnicombe, A. Thompson, Differentiating benign from malignant solid breast masses: value of shear wave elastography according to lesion stiffness combined with greyscale ultrasound according to BI-RADS classification, Br. J. Cancer 107 (2012) 224–229.

[40] A. Evans, P. Whelehan, K. Thomas, D. McLean, K. Brauer, C. Purdie, L. Jordan, L. Baker, A. Thompson, Quantitative shear wave ultrasound elastography: initial experience in solid breast masses, Breast Cancer Res. 12 (2010) R104.

[41] E. Fleury, J.C. Fleury, S. Piato, D.J. Roveda, New elastographic classification of breast lesions during and after compression, Diagn. Interv. Radiol. 15 (2) (2009) 96–103.

[42] M.M. Galloway, Texture analysis using gray level run lengths, Comput. Graphics Image Process 4 (1975) 172–179.

[43] J.L. Gennisson, T. Deffieux, M. Fink, M. Tanter, Ultrasound Elastography: principles and techniques, Diagn. Interv. Imaging 94 (2013) 487–495.

[44] M. Gerlinger, A.J. Rowan, S. Horswell, J. Larkin, D. Endesfelder, E. Gronroos, P. Martinez, N. Matthews, A. Stewart, P. Tarpey, I. Varela, B. Philimore, S. Begum, N.Q. McDonald, A. Butler, D. Jones, K. Raine, C. Latimer, C.R. Santos, M. Nohadani, A.C. Eklund, B. Spencer-Dean, G. Clark, L. Pickering, G. Stamp, M. Gore, Z. Szallasi, J. Downward, A. Futreal, C. Swanton, Intratumoral heterogeneity and branched evolution revealed by multiregion sequencing, N. Engl. J. Med. 366 (2012) 883–892.

[45] D.N. Ghista, Physiological systems numbers in medical diagnosis and hospital cost effective operation, J. Mech. Med. Biol. 4 (2004) 401–418.

[46] D.N. Ghista, Nondimensional physiological indices for medical assessment, J. Mech, Med. Biol. 9 (2009) 643–669.

[47] D.N. Ghista, Applied Biomedical Engineering Mechanics, CRC press, 2009.

[48] Global Burden of Disease Cancer Collaboration, The global burden of cancer, 2013, JAMA Oncol. 1 (2015) 505–527.

[49] A. Goddi, M. Bonardi, S. Alessi, Breast Elastography: a literature review, J Ultrasound15 (2012) 192–198.

[50] M. Golatta, M. Schweitzer-Martin, A. Harcos, S. Schott, C. Gomez, A. Stieber, G. Rauch, C. Domschke, J. Rom, F. Schutz, C. Sohn, J. Heli, Evaluation of virtual touch tissue imaging quantification a new shear wave velocity imaging method for breast lesion assessment by ultrasound, BioMed Res. Int. (2014).

[51] R. Gonzalez, R.E. Woods, Digital Image Processing, 2 ed., Prentice Hall, New York, 2002.

[52] H.M. Gweon, J.H. Youk, E.J. Son, J.A. Kim, Clinical application of qualitative assessment for breast masses in shear-wave elastography, Eur. J. Radiol. 82 (2013) e680–e685.

[53] R.M. Haralick, K. Shanmugam, I.H. Dinstein, Textural features for image classification, IEEE Trans. Syst. Man Cybern. 3 (1973) 610–621.

[54] R.J. Hooley, L.M. Scoutt, L.E. Philpotts, Breast ultrasonography: state of the art, Radiology 268 (2013) 612–659.

[55] R.J. Hooley, K.L. Greenberg, R.M. Stackhouse, J.L. Geisel, R.S. Butler, L.E. Philpotts, Screening US in patients with mammographically dense breasts: initial experience with Connecticute Acte 09-41, Radiology 265 (2012) 59–69.

[56] G.N. Hortobagyi, J. de la G. Salazar, K. Pritchard, D. Amadori, R. Haidinger, C.A. Hudis, H. Khaled, M.C. Liu, M. Martin, M. Namer, J.A. O'shaughnessy, Z.Z. Shen, K.S. Albain, The global breast cancer burden: variations in epidemiology and survival, Clin. Breast Cancer 6 (2005) 391–401.

[57] M.K. Hu, Visual pattern recognition by moment invariants, IRE Trans. Inf. Theory 8 (1962) 179–187.

[58] Z. Huang, J. Leng, Analysis of Hu's moment invariants on image scaling and rotation, 2nd International Conference on Computer Engineering and Technology 7 (2010) 476–480.

[59] Z.H. Huang, W.J. Li, J. Wang, T. Zhang, Face recognition based on pixel-level and feature-level fusion of the top-level's wavelet sub-bands, Inf. Fusion 22 (2015) 95–104.

[60] A. Itoh, E. Ueno, E. Tohno, H. Kamma, H. Takahashi, T. Shiina, M. Yamakawa, T. Matsumura, Breast disease: clinical application of US elastography for diagnosis, Radiology 239 (2006) 341–350.

[61] B. Karimi, A. Krzyzak, Computer-aided system for automatic classification of suspicious lesion in breast ultrasound images, Artif. Intell. Soft Comput. (2014) 131–142.

[62] J. Kaur, R. Kaur, Image denoising for speckle noise reduction in ultrasound images using DWT technique Int, J. Appl. Innov. Eng. Manag. 2 (2013) 384–396.

[63] A. Khan, H. Farooq, Principal Component analysis-linear discriminant analysis feature extractor for pattern recognition, IJCSI Int. J. Comput. Sci. 8 (2011) 267–270.

[64] S. Kim, S.H. Choi, Y. Choi, S.H. Kook, H.J. Park, E.C. Chung, Diagnostic performance of shear wave elastography of the breast according to scanning orientation, J. Ultrasound Med. 33 (2014) 1797–1804.

[65] S.J. Kim, K.H. Ko, H.K. Jung, H. Kim, Shear wave elastography: is it valuable additive method to conventional ultrasound for the diagnosis of small (≤2 cm) breast cancer?, Medicine (Baltimore). 94 (2015) e1540.

[66] M.Y. Kim, N. Cho, A. Yi, H.R. Koo, B.L. Yun, W.K. Moon, Sonoelastography in distinguishing benign from malignant complex breast mass and making the decision to biopsy, Korean J. Radiol. 14 (2013) 559–567.

[67] T. Klotz, V. Boussion, F. Kwiatkowski, V.D.D. Fraissinette, A. Bailly-Glatre, S. Lemery, L. Boyer, Shearwave elastography contribution in ultrasound diagnosis management of breast lesions, Diagn. Interv. Imaging 95 (2014) 813–824.

[68] T.M. Kolb, J. Lichy, J.H. Newhouse, Comparison of the performance of screening mammography, physical examination, and breast US and evaluation of factors that influence them: an analysis of 27, 825 patient evaluations, Radiology 225 (2002) 165–175.

[69] D.B. Kopans, Negative mammographic and US findings do not help exclude breast cancer, Radiology222 (2002) 857–858.

[70] S.B. Kotsiantis, Feature selection for machine learning classification problems: a recent overview, Artif. Intell. Rev. (2011) 42.

[71] T.A. Krouskop, T.M. Wheeler, F. Kallel, B.S. Garra, T. Hall, Elastic moduli of breast and prostate tissues under compression, Ultrason. Imaging 20 (1998) 260–274.

[72] V. Kumar, S. Minz, Feature selection: a literature review, Smart Comput. Rev. 4 (2014) 211–229.

[73] D.T. Larose, KNN. 'Discovering Knowledge in Data: An Introduction to Data Mining, Wiley Interscience, New Jersey, 200490–106.

[74] D.T. Larose, Discovering knowledge in data: an introduction to data mining, Chapter 6: Decision Trees, Wiley Interscience, New Jersey USA, 2004108–126.

[75] S.H. Lee, N. Cho, J.M. Chang, H.R. Koo, J.Y. Kim, W.H. Kim, M.S. Bae, A. Yi, W.K. Moon, Two-view versus single-view shear-wave elastography: comparison of observer performance in differentiating benign from malignant breast masses, Radiology 28 (2013) 130561.

[76] S.H. Lee, J.M. Chang, W.H. Kim, M.S. Bae, N. Cho, A. Yi, H.R. Koo, S.J. Kim, J.Y. Kim, W.K. Moon, Differentiation of benign from malignant solid breast masses: comparison of two-dimensional and three-dimensional shear-wave elastography, Eur. Radiol. 23 (2013) 1015–1026.

[77] S.H. Lee, J.M. Chang, N. Cho, H.R. Koo, A. Yi, S.J. Kim, J.H. Youk, E.J. Son, S.H. Choi, S.H. Kook, J. Chung, E.S. Cha, J.S. Park, H.K. Jung, K.H. Ko, H.Y. Choi, E.B. Ryu, W.K. Moon, Practice guideline for the performance of breast ultrasound elastography, Ultrasonography 33 (2014) 3–10.

[78] S.H. Lee, J.M. Chang, W.H. Kim, M.S. Bae, M. Seo, H.R. Koo, A.J. Chu, H.M. Gweon, N. Cho, W.K. Moon, Added value of shear-wave elastography for evaluation of breast masses detected with screening US imaging, Radiology 273 (2014) 61–69.

[79] S.H. Lee, J.M. Chang, W. Han, H.G. Moon, H.R. Koo, H.M. Gweon, W.H. Kim, D.Y. Noh, W.K. Moon, Shear wave elastography for the detection of residual breast cancer after neoadjuvant chemotherapy, Ann. Surg. Oncol. 22 (2015) 376–384.

[80] B.E. Lee, J. Chung, E.S. Cha, J.E. Lee, J.H. Kim, Role of shear wave elastography in (SWE) complex cystic and solid breast lesions in comparison with conventional ultrasound, Eur. Radiol. 84 (2015) 1236–1241.

[81] H. Liu, H. Motoda, Feature Selection for Knowledge Discovery and Data Mining, Kluwer Academic Publishers, London GB, 1998.

[82] D.D. Li, H.X.L.H. Xu. Guo, X.W. Bo, X.L. Li, R. Wu, J.M. Xu, Y.F. Zhang, K. Zhang, Combination of two-dimensional shear wave elastography with ultrasound breast imaging reporting and data system in the diagnosis of breast lesions: a new method to increase the diagnostic performance, Eur. J. Radiol. (2015) 1–11.

[83] C.M. Lo, Y.C. Lai, Y.H. Chou, R.F. Chang, Quantitative breast lesion classification based on multichannel distributions in shear wave imaging, Comput. Methods Programs Biomed. 122 (2015) 354–361.

[84] S.G. Mallat, A theory for multiresolution signal decomposition: the wavelet representation IEEE Trans, Pattern Anal. Mach. Intell. 11 (1989) 674–693.

[85] R.J. Martis, U.R. Acharya, C.M. Lim, K.M. Mandana, A.K. Ray, C. Chakraborty, Application of higher order cumulant features for cardiac health diagnosis using ECG signals, Int. J. Neural Syst. 23 (2013) 1350014.

[86] A. Marusky, V. Almendro, K. Polyak, Intra-tumoral heterogeneity: a looking glass for cancer?, Nat. Rev. Cancer 12 (2012) 323–334.

[87] E.B. Mendelson, M. Böhm-Vélez, W.A. Berg, et al., ACR BI-RADS® ultrasound, ACR BI-RADS® Atlas, Breast Imaging Reporting and Data System, American College of Radiology, Reston, VA, 2013.

[88] H.S. Mun, S.H. Choi, S.H. Kook, Y. Choi, W.K. Jeong, Y. Kim, Validation of intra- and interobserver reproducibility of shear wave Elastography: phantom study, Ultrasonics 53 (2013) 1039–1043.

[89] K. Nakashima, T. Shiina, M. Sakurai, et al., JSUM ultrasound Elastography practice guidelines: breast, J. Med. Ultrason. 40 (2013) 359–391.

[90] W.L. Ng, K. Rahmat, F. Fadzli, F.I. Rozalli, N.M.S. Mohammad, P.A. Chandran, C.J. Westerhout, A. Vijayanathan, Y.F. Abdul Aziz, Shearwave elastography increases diagnostic accuracy in characterization of breast lesions, Medicine (Baltimore). 95 (2016) e3146.

[91] D.C. Olgun, B. Korkmazer, F. Kilic, A.S. Dikici, M. Velidedeoglu, F. Aydogan, F. Kantarci, M.H. Yilmaz, Use of shear wave elastography to differentiate benign and malignant breast lesions, Diagn. Interv. Radiol. 20 (2014) 239–244.

[92] J.T. Olkkonen, Discrete Wavelet Transforms- Theory and Applications, In-Tech Publisher, 2011.

[93] J. Ophir, I. Cespedes, H. Ponnekanti, Y. Yazdi, X. Li, Elastography: a quantitative method for imaging the elasticity of biological tissues, Ultrason. Imaging 13 (1991) 111–134.

[94] K.J. Opielinski, P. Pruchnicki, T. Gudra, P. Podgorski, J. Kurcz, T. Krasnicki, M. Sasiadek, J. Majewski, Imaging results of multi-modal ultrasound computerized tomography system designed for breast diagnosis, Comput. Med. Imaging Graph. 46 (2015) 83–94.

[95] A.Y. Park, E.J. Son, J.A. Kim, K. Han, J.H. Youk, Lesion stiffness measured by shear-wave Elastography: preoperative predictor of the histologic underestimation of US-guided core needle breast biopsy, Eur. J. Radiol. 84 (2015) 2509–2514.

[96] J. Pohjalainen, S. Kadioglu, O. Rasanen, Feature selection for speaker traits, In: Proc. 13th Annual Conference of the International Speech Communication Association (Interspeech), Portland, Oregon, USA, 2012.

[97] P. Pudil, J. Novovicova, J. Kittler, Floating search methods in feature selection, Pattern Recogn. Lett. 15 (1994) 1119–1125.

[98] B. Ranger, P.J. Littrup, N. Duric, P. Chandiwala-Mody, C. Li, S. Schmidt, J. Lupinacci, Breast ultrasound tomography versus magnetic resonance imaging for clinical display of anatomy and tumor rendering: preliminary results, AJR Am. J. Roentgenol. 198 (2012) 233–239.

[99] P. Ricci, E. Maggini, E. Mancuso, P. Lodise, V. Cantisani, C. Catalano, Clinical application of breast elastography: state of the art, Eur J Radiol 83 (2014) 429–437.

[100] M. Robnik-Sikonja, I. Kononenko, Theoretical and empirical analysis of ReliefF and RReliefF, Mach. Learn. J. 53 (2003) 23–69.

[101] I. Saarenmaa, T. Salminen, U. Geiger, P. Heikkinen, S. Hyvarinen, J. Isola, V. Kataja, M.L. Kokko, R. Kokko, E. Kumpulainen, A. Karkkainen, J. Pakkanen, P. Peltonen, A. Piironen, A. Salo, M.L. Ta, viala, M. Haka, The effect of age and density of the breast on the sensitivity of breast cancer diagnostic by mammography and ultrasonography, Breast Cancer Res. Treat. 67 (2001) 117–123.

[102] A. Sarvazyan, A.R. Skovoroda, S. Emelianov, K.B. Fowlkes, Biophysical bases of elasticity imaging, Acoust Imag 21 (1995) 223–241.

[103] G. Scaperrotta, C. Ferranti, C. Costa, L. Mariani, M. Marchesini, L. Suman, C. Folini, S. Bergonzi, Role of sonoelastography in nonpalpable breast lesions, Eur. Radiol. 18 (2008) 2381–2389.

[104] H.J. Shin, M.J. Kim, H.Y. Kim, Y.H. Roh, M.J. Lee, Comparison of shear wave velocities on ultrasound Elastography between different machines, transducers, and acquisition depth: a phantom study, Eur. Radiol. (2016).

[105] G.N. Srinivasan, G. Shobha, Statistical texture analysis proceedings of world academy of science, Eng. Technol. 36 (2008) 2070–3740.

[106] A.T. Stavros, D. Thickman, C.L. Rapp, M.A. Dennis, S.H. Parker, G.A. Sisney, Solid breast nodules: use of sonography to distinguish between benign and malignant lesions, Radiology 196 (1995) 123–134.
[107] V.K. Sudarshan, M.R.K. Mookiah, U.R. Acharya, V. Chandran, F. Molinari, H. Fujita, K.H. Ng, Application of wavelet techniques for cancer diagnosis using ultrasound images: a review, Comput. Biol. Med. 69 (2016) 97–111.
[108] M. Tanter, J. Bercoff, A. Athanasiou, T. Deffieux, J.L. Gennisson, G. Montaldo, M. Muller, A. Tardivon, M. Fink, Quantitative assessment of breast lesion viscoelasticity: initial clinical results using supersonic shear imaging, Ultrasound Med. Biol. 34 (2008) 1373–1386.
[109] E. Tohno, D.O. Cosgrove, J.P. Sloane, Ultrasound Diagnosis of Breast Disease Churchill Livingstone, London, 1994.
[110] M. Tozaki, S. Isobe, E. Fukuma, Preliminary study of ultrasonographic tissue quantification of the breast using the acoustic radiation force impulse (ARFI) technology, Eur. J. Radiol. 80 (2011) e182–e187.
[111] P.D. Wasserman, Advanced Methods in Neural Computing, Van Nostrand Reinhold, New York, NY, 1993.
[112] World Health Organization (WHO), 2013. Retrieved from, http://www.who.int/cancer/detection/breastcancer/en/index1.html.
[113] S. Xian-Quan, J.L. Li, Q.Y. Li, H. Yan, W. Wen-Bo, T. Jie, Performance of ultrasonic shear wave elastography in assessing bening and malignant breast lesions, Acta Academiae Medicinae Sinicae 37 (2015) 294–299.
[114] J.H. Yoon, H.K. Jung, J.T. Lee, K.H. Ko, Shear-wave Elastography in the diagnosis of solid breast masses: what leads to false-negative or false-positive results, Eur. Radiol. 23 (2013) 2432–2440.
[115] J.H. Youk, E.J. Son, A.Y. Park, J.A. Kim, Shear wave elastography for breast masses: local shear wave speed (m/sec) versus Young modulus (kPa), Ultrasonography 33 (2014) 34–39.
[116] J.H. Youk, E.J. Son, H.M. Gweon, H. Kim, Y.J. Park, J.A. Kim, Comparison of strain and shear wave elastography for the differentiation of benign from malignant breast lesions, combined with B-mode ultrasonography: qualitative and quantitative assessments, Ultrasound Med. Biol. 40 (2014) 2336–2344.
[117] J.H. Youk, H.M. Gweon, E.J. Son, K.H. Han, J.A. Kim, Diagnostic value of commercially available shear wave elastography for breast cancers: integration into BI-RADS classification with subcategories of category 4, Eur. Radiol. 23 (2013) 2695–2704.
[118] W. Yu, S. Chattopadhyay, T.C. Lim, U.R. Acharya, Advances in Therapeutic Engineering, CRC press Taylor and Francis group, Boca Raton, London, New York, 2013.
[119] W. Zhang, A. Becciolini, A. Biggeri, P. Pacini, C.R. Muirhead, Second malignancies in breast cancer patients following radiotherapy: a study in Florence, Italy Breast Cancer Res. 13 (2011) R38.
[120] Y. Zhang, S. Wang, P. Sun, P. Philips, Pathological brain detection based on wavelet entropy and Hu moment invariants, Biomed. Mater. Eng. 26 (2015) 1283–1290.
[121] Q. Zhang, Y. Xiao, S. Chen, C. Wang, H. Zheng, uantification of elastic heterogeneity using contourlet-based texture analysis in shear wave elastography for breast tumor classification, Ultrasound Med. Biol. 41 (2015) 588–600.
[122] B.N. Zhang, X.C. Cao, J.Y. Chen, J. Chen, L. Fu, X.C. Hu, Z.F. Jiang, H.Y. Li, N. Liao, D.G. Liu, O. Tao, Z.M. Shao, Q. Sun, S. Wang, Y.S. Wang, B.H. Xu, J. Zhang, Guidelines on the diagnosis and treatment of breast cancer, Gland Surg. 1 (2012) 39–61.
[123] H. Zhi, X.Y. Xiao, B. Ou, W.J. Zhong, Z.Z. Zhao, X.B. Zhao, H.Y. Yang, B.M. Luo, Could ultrasonic elastography help the diagnosis of small (≤2 cm) breast cancer with the usage of sonographic BI-RADS classification?, Eur. J. Radiol. 81 (2012) 3216–3221.
[124] J.Q. Zhou, W.W. Zhan, C. Chang, X.X. Zhang, Y. Jia, Y.J. Dong, C. Zhou, J. Sun, E.G. Grant, Breast lesions: evaluation with shear wave elastography with shear wave elastography, with special emphasis on the stiff rim sign, Radiology 272 (2014) 63–72.
[125] G. Zografos, D. Koulocheri, P. Liakou, M. Sofras, S. Hadjiagapis, M. Orme, V. Marmarelis, Novel technology of multimodal ultrasound tomography detects breast lesions, Eur. Radiol. 23 (2013) 673–683.
[126] H.M. Zonderland, E.G. Coerkamp, J. Hermans, M.J. van de Vijver, A.E. van Voorthuisen, Diagnosis of breast cancer: contribution of US as an adjunct to mammography, Radiology 213 (1999) 413–422.